# SCIENTIFIC REPORTS

**OPEN**

# Influence of W substitution on crystal structure, phase evolution and microwave dielectric properties of $(Na_{0.5}Bi_{0.5})MoO_4$ ceramics with low sintering temperature

Li-Xia Pang[1], Di Zhou[2,3], Ze-Ming Qi[4] & Zhen-Xing Yue[5]

In this work, the $(Na_{0.5}Bi_{0.5})(Mo_{1-x}W_x)O_4$ (x = 0.0, 0.5 and 1.0) ceramics were prepared via solid state reaction method. All the samples can be well densified at sintering temperature about ~720 °C. Dense and homogeneous microstructure with grain size lying between 2~8 μm can be observed from scanning electron microscopy (SEM). Microwave dielectric permittivity of the $(Na_{0.5}Bi_{0.5})(Mo_{0.5}W_{0.5})O_4$ ceramic was found to be temperature-independent in a wide range between 25~120 °C with a temperature coefficient of frequency (TCF) ~−6 ppm/°C, a permittivity ~28.9, and Qf values 12,000~14,000 GHz. Crystal structure was refined using Rietveld method and lattice parameters are $a = b = 5.281$ (5) Å and $c = 11.550$ (6) Å with a space group I $4_1$/a (88). The $(Na_{0.5}Bi_{0.5})(Mo_{1-x}W_x)O_4$ ceramics might be good candidate for low temperature co-fired ceramics (LTCC) technology.

Microwave dielectric ceramics usually possess large dielectric permittivity ($\varepsilon_r$, compared with that of polymer), small temperature coefficient of frequency (TCF) and low dielectric loss (high quality factor Qf). In recent forty years, microwave dielectric ceramics have been extensively employed as dielectric resonator (DR), dielectric filter, duplexer, dielectric waveguide, dielectric substrate and etc. in mobile communication, radar and global position system (GPS) and other satellite navigation guiding and positioning systems. High integration and miniaturization of modern microwave devices also benefit from the fast development of microwave dielectric materials[1–3].

In the past forty years, large amount of microwave dielectrics have been explored, such as $(Mg,Ca)TiO_3$ system with $\varepsilon_r$~20, $Ba(Mg,Zn)(Ta,Nb)O_3$ system with $\varepsilon_r$~30–40, $(Zr,Sn)TiO_4$ system with $\varepsilon_r$~40–45, $(Sr,Ca)TiO_3$-$(La,Nd)AlO_3$ system with $\varepsilon_r$~45, and $BaO$-$(Sm,Nd)_2O_3$-$TiO_2$ system with $\varepsilon_r$ above 70[4–8]. However, the high sintering temperature of traditional microwave dielectric ceramics are not suitable for the fast developing modern fabrication technology, low temperature co-fired ceramics (LTCC) technology[2, 3]. Although many lead-rich microwave dielectric ceramics possess low sintering temperature, their toxicity has limited their wide application[9–13]. In recent ten years, the so-called ultra-low temperature co-fired ceramics (ULTCC) technology has attracted much attention due to their intrinsic low firing temperature below base metals' melting points, such as Al (~660 °C) and Ag (~961 °C)[14, 15]. The top two biggest ULTCC families are Te-rich and Mo-rich series[14–17]. Considering the environmental friendless and price advantage, Mo-rich ULTCC will play an important role in the high integrated electronic devices. Among them, a big family with scheelite-related structure has attracted much attention. Scheelite structure derive from natural mineral $CaWO_4$ and got its name after the discoverer chemist C.W. Scheele from Sweden. The typical formula of scheelite structure is $ABO_4$, in which A site can be alkali metal ions, alkaline earth metal ions, some trivalent metal ions, such as Li, Na, Ba, Sr, Ca, Bi etc., with eight coordination number and B site can be trivalent, pentavalent or six valence metal ion, such as Fe, Ga V, Mo, W etc., with four

[1]Micro-optoelectronic Systems Laboratories, Xi'an Technological University, Xi'an, 710032, Shaanxi, China. [2]Electronic Materials Research Laboratory, Key Laboratory of the Ministry of Education & International Center for Dielectric Research, Xi'an Jiaotong University, Xi'an, 710049, Shaanxi, China. [3]Department of Materials Science and Engineering, University of Sheffield, Sheffield, S1 3JD, UK. [4]National Synchrotron Radiation Laboratory, University of Science and Technology of China, Anhui, 230029, Hefei, China. [5]State Key Laboratory of New Ceramics and Fine Processing, Department of Materials Science and Engineering, Tsinghua University, Beijing, 100084, PR China. Correspondence and requests for materials should be addressed to D.Z. (email: zhoudi1220@gmail.com)
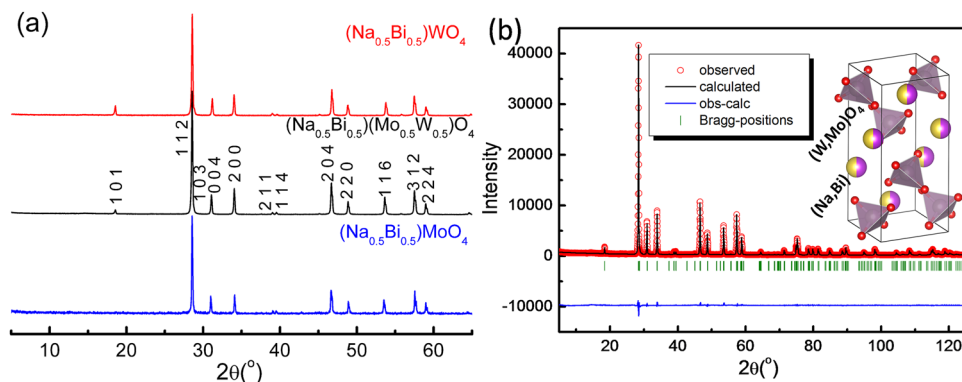
**Figure 1.** XRD patterns of the $(Na_{0.5}Bi_{0.5})(Mo_{1-x}W_x)O_4$ (x = 0.0, x = 0.5 and x = 1.0) ceramics (**a**), the experimental (circles) and simulated (line) XRD patterns of the $(Na_{0.5}Bi_{0.5})(Mo_{0.5}W_{0.5})O_4$ composition sintered at 720 °C using space group I $4_1$/a (88) ($R_p$ = 9.08%, $R_{wp}$ = 9.95%, $R_{exp}$ = 6.25%) (**b**) (The short vertical lines represent Bragg reflection positions. The continuous line at the bottom shows the difference between experimental and simulated intensity).

| Atom | Site | Occ. | x | y | z | Biso |
|------|------|------|---|---|---|------|
| Na | 4b | 0.125 | 0.00000 | 0.25000 | 0.62500 | 0.75528 |
| Bi | 4b | 0.125 | 0.00000 | 0.25000 | 0.62500 | 0.75528 |
| Mo | 4a | 0.125 | 0.00000 | 0.25000 | 0.12500 | 0.60363 |
| W | 4a | 0.125 | 0.00000 | 0.25000 | 0.12500 | 0.60363 |
| O | 16 f | 1.000 | 0.1491(9) | 0.0041(1) | 0.2089(5) | 0.75169 |

**Table 1.** Refined atomic fractional coordinates from XRD data of the $(Na_{0.5}Bi_{0.5})(Mo_{0.5}W_{0.5})O_4$ ceramic and the cell parameters are a = b = 5.281 (5) Å, c = 11.550 (6) Å with a space group is I $4_1$/a (88).

coordination number[18]. Meanwhile, the anion O can also be replaced partially by F or N. Scheelite structure is quite adaptive like perovskite structure in $ABO_3$ systems. High concentration as large as 1/3 of defects can be introduced into scheelite structure's A site, in which the formula can be written as $A_{1-x}\Phi_xMoO_4$. Defects and substitutions can cause the ordering at A site, such as $(K_{0.5}Eu_{0.5})MoO_4$ and $Bi_{2/3}\Phi_{1/3}MoO_4$[19–24]. As reported in literatures, large difference of ionic radius at B site also results in the ordering of $[BO_4]$ arrangement at B site, such as $Bi(Fe_{1/3}Mo_{2/3})O_4$[25]. High adaptability of scheelite structure can provide large amount of data to study its structure-property relation. In 2006 and 2007[26, 27], Hong et al. first reported microwave dielectric properties and sintering behaviors of the scheelite structured $(Ca,Sr,Ba)(W,Mo)O_4$ ceramics with sintering temperature below 1100 °C, dielectric permittivity between 8~11, Qf values between 30,000 GHz~90,000 GHz, TCF values between −40~−80 ppm/°C. Large negative TCF values limit their application. Subsequently, a series of A site complex substitutions compositions with scheelite structure were reported to possess positive TCF values in our previous work, such as the $(Li_{0.5}Bi_{0.5})MoO_4$ ($\varepsilon_r$ = 44.4, Qf = 3,200 GHz and TCF = +245 ppm/°C), $(Na_{0.5}Bi_{0.5})MoO_4$ ($\varepsilon_r$ = 34.4, Qf = 12,300 GHz and TCF = +43 ppm/°C) and $(Ag_{0.5}Bi_{0.5})MoO_4$ ($\varepsilon_r$ = 30, Qf = 12,600 GHz and TCF = +57 ppm/°C)[28, 29]. When the B site is occupied by W, the $(Li_{0.5}Bi_{0.5})WO_4$ and $(Ag_{0.5}Bi_{0.5})WO_4$ compositions crystallize in wolframite structure[30] and only the $(Na_{0.5}Bi_{0.5})WO_4$ still keep scheelite structure[31]. These results offer the opportunity to design temperature stable scheelite structured microwave dielectric ceramics and study the relation between structure and TCF values. Besides the wide range adjustability of permittivity, Qf and TCF values, low sintering temperature below 700 °C is also a highlight for the Mo-based scheelite materials. In the present work, phase evolution, crystal structure, microstructure, microwave dielectric properties and their relation in the $(Na_{0.5}Bi_{0.5})(Mo_{1-x}W_x)O_4$ (x = 0.0, 0.5 and 1.0) system were studied in detail.

XRD patterns of the $(Na_{0.5}Bi_{0.5})(Mo_{1-x}W_x)O_4$ (x = 0.0, 0.5 and 1.0) ceramics sintered at 720 °C for 2 h are presented in Fig. 1(a). All the samples crystallized in standard tetragonal scheelite structure, in which $Na^+$ and $Bi^{3+}$ randomly occupied 8-coordinated A site and $Mo^{6+}$ and $W^{6+}$ randomly occupied 4-coordinated B site. This result is similar to the literatures' reports[32–34]. This result indicates that tetragonal scheelite structured solid solution was formed in full composition range in the $(Na_{0.5}Bi_{0.5})(Mo_{1-x}W_x)O_4$ ceramics. To study the crystal structure details of x = 0.5 composition, refinements were performed by using Fullprof software[35] based on refined XRD data. Measured and calculated XRD patterns are presented in Fig. 1(b). As listed in Table 1, refined cell parameters are a = b = 5.281 (5) Å and c = 11.550 (6) Å. with a space group I4$_1$/a (No. 88) and acceptable $R_p$ = 9.08%, $R_{wp}$ = 9.95% and $R_{exp}$ = 6.25% using the data (ICSD #67491) reported by Teller as starting model[36]. Cell parameters of the $(Na_{0.5}Bi_{0.5})MoO_4$ and $(Na_{0.5}Bi_{0.5})WO_4$ are a = b = 5.274 (4) Å, c = 11.578 (2) Å and a = b = 5.282 Å, c = 11.50 Å, respectively, as reported by Hanuza, Waskowska et al.[31, 37, 38]. In scheelite structure, $Mo^{6+}$ is 4-coordinated and its ionic radius is 0.41 Å, while the ionic radius of $W^{6+}$ is 0.60 Å[39]. Hence it is understandable that cell parameters changed almost linearly with $W^{6+}$ substitution concentration.
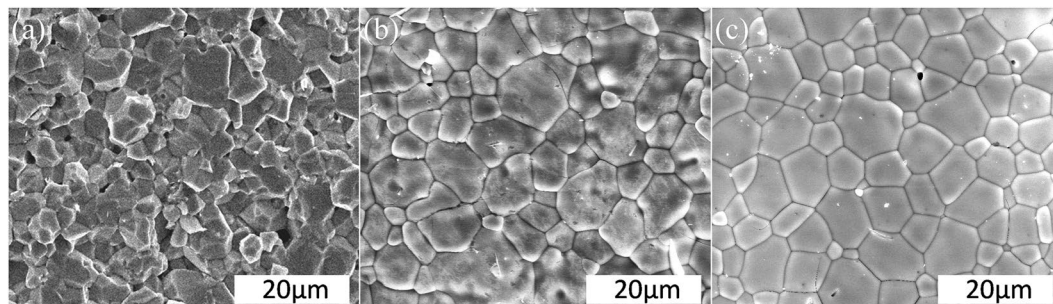
**Figure 2.** SEM images of the $(Na_{0.5}Bi_{0.5})(Mo_{1-x}W_x)O_4$ (**a**) x = 0.0 (fractured surface), (**b**) x = 0.5 and (**c**) x = 1.0 ceramics sintered at 720 °C for 2 hr.

| Composition | Phase | S.T. (°C) | $\varepsilon_r$ | Qf (GHz) | TCF (ppm/°C) | A site radius | B site Radius | Refs |
|---|---|---|---|---|---|---|---|---|
| $(Li_{0.5}Bi_{0.5})MoO_4$ | scheelite | 560 | 44.4 | 3,200 | +245 | 1.045 | 0.41 | 28 |
| $(Li_{0.5}Bi_{0.5})(Mo_{0.4}W_{0.6})O_4$ | composite | 620 | 31.5 | 8,500 | +20 | 1.045 | 0.416 | 30 |
| $(Li_{0.5}Bi_{0.5})WO_4$ | wolframite | 740 | 27.2 | 17,000 | −56 | 1.045 | 0.42 | 30 |
| $(Na_{0.5}Bi_{0.5})MoO_4$ | scheelite | 690 | 34.4 | 12,300 | +43 | 1.175 | 0.41 | 29 |
| $(Na_{0.5}Bi_{0.5})(Mo_{0.5}W_{0.5})O_4$ | scheelite | 720 | 28.9 | 14,000 | −6 | 1.175 | 0.415 | this work |
| $(Na_{0.5}Bi_{0.5})WO_4$ | scheelite | 720 | 25.7 | 17,500 | −18 | 1.175 | 0.42 | this work |
| $(Ag_{0.5}Bi_{0.5})MoO_4$ | scheelite | 690 | 30.4 | 12,600 | +57 | 1.225 | 0.41 | 29 |
| $(Ag_{0.5}Bi_{0.5})(Mo_{0.5}W_{0.5})O_4$ | scheelite | 580 | 26.3 | 10,000 | +20 | 1.225 | 0.415 | 40 |
| $(Ag_{0.5}Bi_{0.5})WO_4$ | wolframite | 580 | 35.9 | 13,000 | −69 | 1.225 | 0.42 | 41 |
| $(K_{0.5}Bi_{0.5})MoO_4$ | monoclinic | 630 | 37 | 4,000 | +117 | 1.34 | 0.41 | 29 |

**Table 2.** Phase compositions, sintering temperatures (S. T.) and Microwave dielectric properties of the $(A_{0.5}Bi_{0.5})(Mo,W)O_4$ (A = Li, Na, K and Ag) ceramics.

Microstructures of the $(Na_{0.5}Bi_{0.5})(Mo_{1-x}W_x)O_4$ (x = 0.0, 0.5 and 1.0) ceramics sintered at 720 °C for 2 h are shown in Fig. 2. Dense and homogeneous microstructure can be observed, which means that all the ceramics could be well densified at a low sintering temperature ~720 °C. There is no apparent change trend of grains versus substitution of W and it lied between 2~8 μm.

Phase compositions, sintering temperatures and microwave frequency dielectric properties of the $(A_{0.5}Bi_{0.5})$ $(Mo,W)O_4$ (A = Li, Na and Ag) ceramics were listed in Table 2 [28–30, 40, 41]. The microwave dielectric properties of $(Na_{0.5}Bi_{0.5})WO_4$ were first reported here with a $\varepsilon_r$~25.7, a Qf value ~17,500 GHz and a $\tau_f$ value ~− 18 ppm/°C. Although the permittivity of $(Na_{0.5}Bi_{0.5})WO_4$ ceramic is a little smaller than that of $(Na_{0.5}Bi_{0.5})MoO_4$ ceramic, its Qf value is 1.4 times larger than that of the $(Na_{0.5}Bi_{0.5})MoO_4$ ceramic. It must be noted that their TCF values are opposite and this provides an opportunity to design a temperature stable $(Na_{0.5}Bi_{0.5})(Mo_{0.5}W_{0.5})O_4$ solid solution ceramic with a $\varepsilon_r$~28.9, a Qf value ~14,000 GHz and a $\tau_f$ value ~−6 ppm/°C as listed in Table 2. As mentioned above, full solid solution can be formed in the $(Na_{0.5}Bi_{0.5})(Mo_{1-x}W_x)O_4$ ceramics. It is quite different from the situation in $(Li_{0.5}Bi_{0.5})(Mo_{1-x}W_x)O_4$ system, in which composite samples were formed. Besides, it is also quite different from the situation in $(Ag_{0.5}Bi_{0.5})(Mo_{1-x}W_x)O_4$ system, in which limited solid solution were formed. Compared with composite method, solid solution method is more controllable. Change of permittivity might be explained by Shannon's additive rule[42]. According to Shannon's results, the polarizabilities $\alpha_x$ of $(Na_{0.5}Bi_{0.5})$ $(Mo_{1-x}W_x)O_4$ could be calculated as follows:

$$\alpha_x = 0.5 \times (\alpha_{Bi^{3+}} + \alpha_{Na^+}) + x\alpha_{W^{6+}} + (1 - x)\alpha_{Mo^{6+}} + 4\alpha_{O^{2-}} \tag{1}$$

where $\alpha_{Bi^{3+}}, \alpha_{O^{2-}}, \alpha_{Mo^{6+}}, \alpha_{Na^+}$ and $\alpha_{W^{6+}}$ are the polarizabilities of $Bi^{3+}$, $O^{2-}$, $Mo^{6+}$, $Na^+$ and $W^{6+}$, respectively[26, 27, 42]. Using the Clausius-Mossotti relation, the relation between dielectric permittivity $\varepsilon_r$, polarizability $\alpha_x$, cell volume $V_x$, and the dielectric constant are obtained as following:

$$\varepsilon_x = \frac{3V_x + 8\pi\alpha_x}{3V_x - 4\pi\alpha_x} \Leftrightarrow \alpha_x = \frac{3V_x}{4\pi}\frac{\varepsilon_x - 1}{\varepsilon_x + 2} \tag{2}$$

in which $V_x$ is cell volume and $\varepsilon_x$ is the permittivity of $(Na_{0.5}Bi_{0.5})(Mo_{1-x}W_x)O_4$ ceramics. The calculated molecular polarzabilites from equations (1) and (2) and macroscopical microwave dielectric properties were listed in Table 3. Because the ionic polarizability of $Mo^{6+}$ is larger than that of $W^{6+}$, it is understandable that permittivity decreased with increase of W content. The relative error of molecular polarzability is below 13%, which is acceptable and might be attributed to the specific ion neighboring environment. To better understand the scheelite solid solubility here, the phase compositions, sintering temperatures and microwave dielectric properties of the $(A_{0.5}Bi_{0.5})(Mo,W)O_4$ (A = Li, Na, K and Ag) ceramics are presented in Table 2 in order of ionic radius of $A^+$. It is

| Composition | $\varepsilon_r$ | Cell volume ($Å^3$) | $\alpha_{meas}$ ($Å^3$) | $\alpha_{cal}$ ($Å^3$) | Ref. |
|---|---|---|---|---|---|
| $(Na_{0.5}Bi_{0.5})MoO_4$ | 34.4 | 322.09/4 | 17.639 | 15.28 | 17 |
| $(Na_{0.5}Bi_{0.5})(Mo_{0.5}W_{0.5})O_4$ | 28.9 | 322.20/4 | 17.363 | 15.24 | this work |
| $(Na_{0.5}Bi_{0.5})WO_4$ | 25.7 | 319.80/4 | 17.019 | 15.2 | this work |

**Table 3.** Dielectric permittivity, cell volume, calculated and measured molecular polarizability of the $(Na_{0.5}Bi_{0.5})$ $(Mo_{1-x}W_x)O_4$ ceramics.
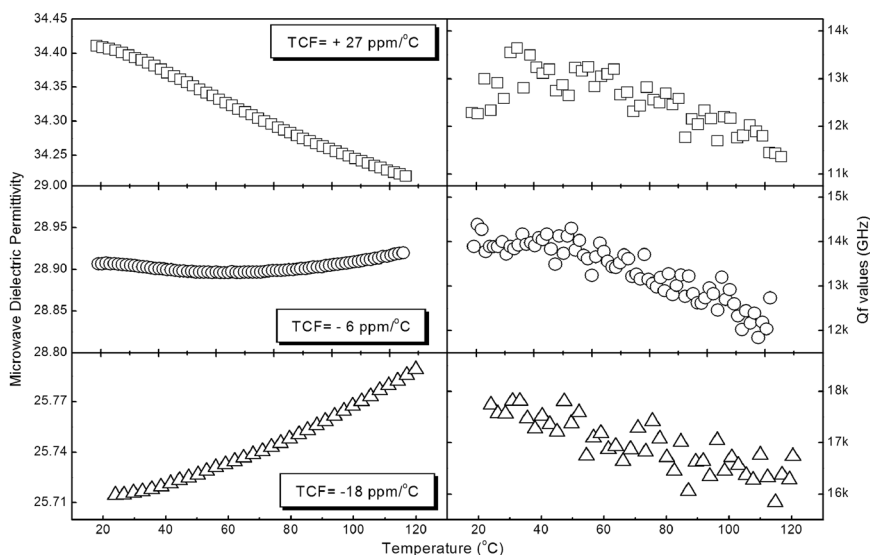


**Figure 3.** Microwave dielectric permittivities and Qf values of the $(Na_{0.5}Bi_{0.5})(Mo_{1-x}W_x)O_4$ (x = 0, 0.5, 1.0) ceramics as a function of temperature.

seen that the scheelite solid solubility is influenced both by the equivalent ionic radius on A and B sites. According to our previous work, scheelite solid solubility is less than 40% in the $(Li_{0.5}Bi_{0.5})(Mo_{1-x}W_x)O_4$ system and possibly larger than 50% in the $(Ag_{0.5}Bi_{0.5})(Mo_{1-x}W_x)O_4$ system, while scheelite solid solution was formed in the whole composition range in $(Na_{0.5}Bi_{0.5})(Mo_{1-x}W_x)O_4$ system here. According to Errandonea and Manjon' review ref. 43, structures of $ABX_4$ materials are determined both by the ionic radius of A, B, and X ions and the pressure. It is not easy to give a simple structural factor for scheelite structure, such as the famous tolerance factor defined as $(R_A + R_O)/(R_B + R_O)$ in perovskite structure[44]. Anyway, from the experimental data listed in Table 2, we can only give a conclusion that scheelite structure can only be kept within a limited range of radius of ions on both A and B sites in oxides. The microwave dielectric permittivities and Qf values of $(Na_{0.5}Bi_{0.5})(Mo_{1-x}W_x)O_4$ (x = 0, 0.5, 1.0) ceramics as a function of temperature are shown in Fig. 3. It is clearly seen that substitution of W for M in the $(Na_{0.5}Bi_{0.5})MoO_4$ ceramic efficiently modify the temperature dependence of permittivity. In a wide temperature range 20~120 °C, the permittivity of $(Na_{0.5}Bi_{0.5})(Mo_{0.5}W_{0.5})O_4$ ceramic changed slightly around 28.9, while Qf values above 12,000 GHz. It is interesting to note that no matter in forms of solid solution or composite, TCF values can be easily tailored to be near zero in the $(A_{0.5}Bi_{0.5})(Mo,W)O_4$ (A = Li, Na, K and Ag) systems, which makes them possible in fabrication of temperature stable devices. Infrared reflectivity fitting was also employed to study the intrinsic dielectric properties and details were presented in Supplemental Information. $Bi^{3+}$ neighboring structure was found to account for the shift of macroscopical permittivity due to the large polarization ~6.12 $Å^3$, which is larger than that of $Mo^{6+}$ and $W^{6+}$ ions (3.28 and 3.2 $Å^3$, respectively)[26, 27, 42].

## Summary

Different from the $(Li_{0.5}Bi_{0.5})(Mo,W)O_4$ and $(Ag_{0.5}Bi_{0.5})(Mo,W)O_4$ system, with a ionic radius of 1.18 Å ($Na^+$) between that of $Li^+$ and $Ag^+$, $(Na_{0.5}Bi_{0.5})(Mo,W)O_4$ system can easily crystallize in standard scheelite structure. Crystal structure refinement based on Rietveld method gave the cell parameters a = b = 5.281 (5) Å, and c = 11.550 (6) Å with a space group I $4_1$/a (88). With increase of W content, microwave permittivity decreased from 34.4 to 25.7 and Qf value increased from 12,300 GHz to 17,500 GHz while TCF shifting from +43 to −18 ppm/°C, which indicates that TCF value is strongly dependent on the $[BO_4]$ tetrahedron in scheelite structure. Far-infrared reflectivity further confirmed that phonons at infrared region contributed main dielectric polarization at microwave region. The $(Na_{0.5}Bi_{0.5})(Mo,W)O_4$ system could be good candidate for Pb-free ULTCC technology.

## Methods

**summary.** The $(Na_{0.5}Bi_{0.5})(Mo_{1-x}W_x)O_4$ (x = 0.0, 0.5 and 1.0) ceramics were prepared via the traditional solid state reaction method as described in our previous work[2, 15]. The calcination temperature is 600 °C and the samples were sintered under air atmosphere in 700~740 °C. XRD was performed using a Rigaku D/MAX-2400 X-ray diffractometry with Cu Kα radiation. The Rietveld profile refinement method was performed on chosen resutls, using Fullprof program[35]. Ceramic surfaces were examined by a FEI Quanta 250 F scanning electron microscopy (SEM). Infrared reflectivity spectra were collected using a Bruker IFS 66 v FTIR spectrometer (on Infrared beamline station (BL01B) at National Synchrotron Radiation Laboratory (NSRL), China). Microwave frequency dielectric properties were obtained using the $TE_{01\delta}$ dielectric resonator method[45] with a HP 8720 Network Analyzer and a thermal cycling chamber (Delta 9023, Delta Design, Poway, CA). The temperature coefficient of frequency TCF ($\tau_f$) was obtained using the following formula:

$$TCF(\tau_f) = \frac{f_T - f_{T_0}}{f_{T_0} \times (T - T_0)} \times 10^6$$

(3)

where the $f_T$ and $f_{T0}$ were the $TE_{01\delta}$ frequencies at temperature T and $T_0$, respectively.

## References

1. Mirsaneh, M., Leisten, O. P., Zalinska, B. & Reaney, I. M. Circularly Polarized Dielectric-Loaded Antennas: Current Technology and Future Challenges. *Adv. Funct. Mater.* **18**, 2293–2300 (2008).
2. Zhou, D. *et al.* Novel temperature stable high-εr microwave dielectrics in the Bi$_2$O$_3$–TiO$_2$–V$_2$O$_5$ system. *J. Mater. Chem. C.* **4**, 5357–5362 (2016).
3. Sebastian, M. T. & Jantunen, H. Low Loss Dielectric Materials for LTCC Applications: A Review. *Int. Mater. Rev.* **53**, 57–90 (2008).
4. Chu, L. W., Hsiue, G. H. & Lin, I. N. Synthesis of Ba$_2$Ti$_9$O$_{20}$ materials via a dissolution–precipitation mechanism in a hydrothermal process. *Acta Mater.* **54**, 1671–1677 (2006).
5. Scotta, R. I., Thomas, M. & Hampson, C. Development of low cost, high performance Ba(Zn$_{1/3}$Nb$_{2/3}$)O$_3$ based materials for microwave. *J. Eur. Ceram. Soc.* **23**, 2467–2471 (2003).
6. Hirano, S., Hayashi, T. & Hattori, A. Chemical Processing and Microwave Characteristics of (Zr,Sn)TiO$_4$ Microwave Dielectrics. *J. Am. Ceram. Soc.* **74**, 1320–1324 (1991).
7. Jancar, B., Suvorov, D., Valant, M. & Drazic, G. Characterization of CaTiO$_3$-NdAlO$_3$ dielectric ceramics. *J. Eur. Ceram. Soc.* **23**, 1391–1400 (2003).
8. Wu, Y. J. & Chen, X. M. Modified Ba$_{6-3x}$Nd$_{8+2x}$Ti$_{18}$O$_{54}$ microwave dielectric ceramics. *J. Eur. Ceram. Soc.* **19**, 1123–1126 (1999).
9. Kucheiko, S., Choi, J. W., Kim, H. J., Yoon, S. J. & Jung, H. J. Microwave Characteristics of (Pb,Ca)(Fe,Nb,Sn)O$_3$ Dielectric Materials. *J. Am. Ceram. Soc.* **80**, 2937–2940 (1997).
10. Yoon, K. H., Kim, E. S. & Jeon, J. S. Understanding the microwave dielectric properties of (Pb$_{0.45}$Ca$_{0.55}$)[Fe$_{0.5}$(Nb$_{1-x}$Ta$_x$)$_{0.5}$]O$_3$ Ceramics via the bond valence. *J. Eur. Ceram. Soc.* **23**, 2391–2396 (2003).
11. Varghese, J. *et al.* Structural, Dielectric, and Thermal Properties of Pb Free Molybdate Based Ultralow Temperature Glass. *ACS Sustainable Chem. Eng.* **4**, 3897–3904 (2016).
12. Menad, N., Guignot, S. & Houwelingen, J. A. van New Characterization Method of Electrical and Electronic Equipment Wastes (WEEE). *Waste Manage.* **33**, 706–713 (2013).
13. Xiong, T. *et al.* Single Precursor Mediated-Synthesis of Bi Semimetal Deposited N-Doped (BiO)$_2$CO$_3$ Superstructures for Highly Promoted Photocatalysis. *ACS Sustainable Chem. Eng.* **4**, 2969–2979 (2016).
14. Kwon, D. K., Lanagan, M. T. & Shrout, T. R. Microwave dielectric properties and low-temperature cofiring of BaTe$_4$O$_9$ with aluminum metal electrode. *J. Am. Ceram. Soc.* **88**, 3419–3422 (2005).
15. Zhou, D. *et al.* Microwave Dielectric Properties of Li$_2$(M$^{2+}$)$_2$Mo$_3$O$_{12}$ and Li$_3$(M$^{3+}$)Mo$_3$O$_{12}$ (M = Zn, Ca, Al, and In) Lyonsite-Related-Type Ceramics with Ultra-Low Sintering Temperatures. *J. Am. Ceram. Soc.* **94**, 802–805 (2011).
16. Kahari, H., Teirikangas, M., Juuti, J. & Jantunen, H. Improvements and Modifications to Room-Temperature Fabrication Method for Dielectric Li$_2$MoO$_4$ Ceramics. *J. Am. Ceram. Soc.* **98**, 687–689 (2015).
17. Sebastian, M. T., Ubic, R. & Jantunen, H. Low-Loss Dielectric Ceramic Materials and Their Properties. *Int. Mater. Rev.* **60**, 392–412 (2015).
18. Sleight, A. W. & Linn, W. J. Olefin Oxidation Over Oxide Catalysts with the Scheelite Structure. *Ann. N. Y. Acad. Sci.* **272**, 22–44 (1976).
19. Brixner, L. H., Sleight, A. W. & Licis, M. S. Cell dimensions of the molybdates La$_2$(MoO$_4$)$_3$, Ce$_2$(MoO$_4$)$_3$, Pr$_2$(MoO$_4$)$_3$, and Nd$_2$(MoO$_4$)$_3$. *J. Solid State Chem.* **5**, 247–249 (1972).
20. Jeitschko, W. Crystal structure of La$_2$(MoO$_4$)$_3$, a new ordered defect Scheelite type. *Acta Crystallogr., Sect. B: Struct. Crystallogr. Cryst. Chem.* **29**, 2074–2081 (1973).
21. Zhou, D. *et al.* Phase evolution and microwave dielectric properties of xBi$_{2/3}$MoO$_4$-(1−x)BiVO$_4$ (0.0 ≤ x ≤ 1.0) low temperature firing ceramics. *Dalton Trans.* **43**, 7290–7297 (2014).
22. Li, W. B. *et al.* Infrared reflectivity and microwave dielectric properties of (Na$_{0.5}$La$_{0.5}$)MoO$_4$–(Na$_{0.5}$Bi$_{0.5}$)MoO$_4$ ceramics. *J. Am. Ceram. Soc.* **99**, 2083–2088 (2016).
23. Pang, L. X. *et al.* Structure–property relationships of low sintering temperature scheelite-structured (1−x)BiVO$_4$–xLaNbO$_4$ microwave dielectric ceramics. *J. Mater. Chem. C* **5**, 2695–2701 (2017).
24. Zhou, D. *et al.* Phase transition, Raman spectra, infrared spectra, band gap and microwave dielectric properties of low temperature firing (Na$_{0.5x}$Bi$_{1-0.5x}$)(Mo$_x$V$_{1-x}$)O$_4$ solid solution ceramics with scheelite structure. *J. Mater. Chem. C* **21**, 18412–18420 (2011).
25. Sleight, A. W. & Jeitschko, W. Bi$_3$(FeO$_4$)(MoO$_4$)$_2$ and Bi$_3$(GaO$_4$)(MoO$_4$)$_2$-new compounds with scheelite related structures. *Mater. Res. Bull.* **9**, 951–954 (1974).
26. Choi, G. K., Kim, J. R., Yoon, S. H. & Hong, K. S. Microwave Dielectric Properties of Scheelite (A = Ca, Sr, Ba) and Wolframite (A = Mg, Zn, Mn) AMoO$_4$ Compounds. *J. Eur. Ceram. Soc.* **27**, 3063–3067 (2007).
27. Yoon, S. H., Kim, D. W. & Cho, S. Y. Investigation of the relations between structure and microwave dielectric properties of divalent metal tungstate compounds. *J. Eur. Ceram. Soc.* **26**, 2051–2054 (2006).
28. Zhou, D., Randall, C. A., Wang, H., Pang, L. X. & Yao, X. Microwave dielectric ceramics in Li$_2$O-Bi$_2$O$_3$-MoO$_3$ system with ultra low sintering temperatures. *J. Am. Ceram. Soc.* **93**, 1096–1100 (2010).
29. Zhou, D. *et al.* Microwave dielectric properties of (ABi)$_{1/2}$MoO$_4$ (A = Li, Na, K, Rb, Ag) type ceramics with ultra-low firing temperatures. *Mater. Chem. Phys.* **129**, 688–692 (2011).
30. Zhou, D. *et al.* Phase evolution and microwave dielectric properties of (Li$_{0.5}$Bi$_{0.5}$)(W$_{1-x}$Mo$_x$)O$_4$ (0.0 ≤ x ≤ 1.0) ceramics with ultra-low sintering temperatures. *Func. Mater. Lett.* **5**, 1250042 (2012).
31. Hanuza, J. *et al.* Structure and vibrational dynamics of tetragonal NaBi(WO$_4$)$_2$ scheelite crystal. *Vib. Spectr.* **12**, 25–36 (1996).

32. Waskowska, A. *et al.* Low-temperature and high-pressure structural behaviour of NaBi (MoO$_4$)$_2$ - an X-ray diffraction study. *J. Solid State Chem.* **178**, 2218–2224 (2005).
33. Zhou, D., Li, W. B., Xi, H. H., Pang, L. X. & Pang, G. S. Phase composition, crystal structure, infrared reflectivity and microwave dielectric properties of temperature stable composite ceramics (scheelite and zircon-type) in BiVO$_4$–YVO$_4$ system. *J. Mater. Chem. C* **3**, 2582–2588 (2015).
34. Hanuza, J., Maczka, M. & van der Maas, J. H. Polarized IR and Raman spectra of tetragonal NaBi(WO$_4$)$_2$, NaBi(MoO$_4$)$_2$ and LiBi(MoO$_4$)$_2$ single crystals with scheelite structure. *J. Mol. Struc.* **348**, 349–352 (1995).
35. Rodriguez-Carvajal, J. Recent advances in magnetic structure determination by neutron powder diffraction. *J. Physica B.* **192**, 55–59 (1993).
36. Teller, R. G. Refinement of some Na$_{0.5-x}$M'$_{0.5+x/3}$□$_{2x/3}$MoO$_4$, M' = Bi, Ce, La, scheelite structures with powder neutron and X-ray diffraction data. *Acta Crystallogr. Sect. C* **48**, 2101–214 (1992).
37. Klevtsov, P. V., Vinokurov, V. A. & Klevtsova, R. F. Double Molybdates and Tunstates of Alkali-metals with Bismuth M$^+$Bi(TO$_4$)$_2$. *Kristallogr.* **18**, 1192–1197 (1973).
38. Ma, C. *et al.* The novel phase transition of NaBi(WO$_4$)$_2$ under high pressure. *J. Solid State Chem.* **200**, 246–250 (2013).
39. Shannon, R. D. Revised effective ionic radii and systematic studies of interatomic distances in halides and chalcogenides. *Acta Cryst.* **A32**, 751–767 (1976).
40. Zhou, D. *et al.* Structure, Phase Evolution, and Microwave Dielectric Properties of (Ag$_{0.5}$Bi$_{0.5}$)(Mo$_{0.5}$W$_{0.5}$)O$_4$ Ceramic with Ultra low Sintering Temperature. *Inor. Chem.* **53**, 5712–5716 (2014).
41. Zhou, D. *et al.* Crystal structure and microwave dielectric properties of a novel ultra-low temperature fired (AgBi)$_{0.5}$WO$_4$ ceramic. *Eur. J. Inor. Chem.* **2**, 296–301 (2014).
42. Shannon, R. D. Dielectric polarizabilities of ions in oxides and fluorides. *J. Appl. Phys.* **73**, 348–366 (1993).
43. Errandonea, D. & Manjon, F. J. Pressure effects on the structural and electronic properties of ABX$_4$ scintillating crystals. *Progress Mater. Sci.* **53**, 711–773 (2008).
44. Reaney, I. M., Colla, E. L. & Setter, N. Dielectric and structural characteristics of Ba-and Sr-based complex perovskites as a function of tolerance factor. *J. J. Appl. Phys.* **33**(7R), 3984–3990 (1994).
45. Krupka, J., Derzakowski, K., Riddle, B. & Baker-Jarvis, J. A dielectric resonator for measurements of complex permittivity of low loss dielectric materials as a function of temperature. *Meas. Sci. Technol.* **9**, 1751–1756 (1998).

## Acknowledgements

## Author Contributions

L.X.P. and D.Z. prepared the ceramic samples used in the measurement. L.X.P., Z.M.Q. and Z.X.Y. performed experiments and analyzed the data. D.Z., L.X.P., Z.M.Q. and Z.X.Y. discussed the results and contributed to the manuscript. All authors reviewed the manuscript.

## Additional Information

**Supplementary information** accompanies this paper at doi:10.1038/s41598-017-03620-0

**Competing Interests:** The authors declare that they have no competing interests.

**Publisher's note:** Springer Nature remains neutral with regard to jurisdictional claims in published maps and institutional affiliations.